Volume 1 | Number 1 | Jan 2013 | Pages 1–100

Green Chemistry

Cutting-edge research for a greener sustainable future

www.rsc.org/greenchem

Stille couplings in water @RT

ROYAL SOCIETY OF CHEMISTRY

ROYAL SOCIETY OF CHEMISTRY

www.rsc.org/greenchem

Journal Name

ARTICLE

A dual-walled cage MOF as an efficient heterogeneous catalyst for the conversion of CO_2 under mild and co-catalyst free conditions

Yun-Hu Han,[a, b] Zhong-Yuan Zhou,[a, c] Chong-Bin Tian [a] and Shao-Wu Du*[a]

A novel 3D→3D interpenetrated Zn-polyhedral MOF [Zn$_6$(TATAB)$_4$(DABCO)$_3$(H$_2$O)$_3$]·12DMF·9H$_2$O (**1**) (H$_3$TATAB = 4,4',4''-*s*-triazine-1,3,5-triyl-tri-*p*-aminobenzoic acid, DABCO = 1,4-diazabicyclo[2.2.2]octane) based on a dual-walled icosahedral cage has been assembled by incorporating zinc paddlewheel units with nitrogen-rich tritopic carboxylate ligands. Owing to the high density of Lewis acid active sites and affinity to CO_2 of the cage, this material exhibits excellent catalytic efficiency in the cycloaddition of propylene oxide with CO_2 into propylene carbonate under mild conditions (100 °C and ambient CO_2 pressure) with a high yield of 99% over 16 h. Moreover, the catalytic reaction is friendly to environment without any need for co-catalysts and solvents.

Introduction

The development of efficient, environmental-friendly catalysts for CO_2 transformation into economically competitive products has been a longstanding goal for chemists, because CO_2 is inexpensive and an abundant renewable C1 feedstock.[1, 4f] However, CO_2 is also a significant risk to the global climate. There are several possible approaches to reduce the levels of CO_2 in the atmosphere which include removal of CO_2 from air or post-combustion industrial point sources (i.e. flue-gas capture) and transform it into desirable products.[2] A promising strategy for CO_2 fixation is the coupling with epoxides to form five-membered cyclic carbonates, which are valuable chemicals currently used in numerous applications such as electrolyte components in lithium batteries, and intermediates for the production of plastics, pharmaceuticals, polar aprotic solvents, and fine chemicals.[3] Although some homogeneous catalysts have been used for the formation of cyclic carbonates in industry under mild conditions, catalyst separation and disposal presents both environmental and economic drawbacks.[4] Meanwhile, heterogeneous catalysts e.g. metal oxides, zeolites, titanosilicates, and ion-exchanged resins have also been explored to catalyse the cycloaddition of CO_2 with epoxides.[5] However, those catalytic reactions are usually performed under high temperatures (>100°C) and/or CO_2

pressures (>30 atm of CO_2), which increase the cost of reaction processes and energy loss.[5] Therefore, to explore high efficiency heterocatalysis for the coupling reactions of epoxides with CO_2 under mild conditions is a priority to minimize costs and reduce environmental pollution.

Metal-organic frameworks (MOFs), in particular those composed of high-connectivity metal-organic polyhedral cages have recently shown great potential for CO_2 chemical conversion. Polyhedral MOFs have unique advantages including the available control of pore shape and dimensionality, tailored chemical environment and extra-large surface area.[6] Most importantly, these materials contain confined nanospace that allows the facile access of substrates to the catalytically active sites located within the cage.[7] Although several polyhedral MOFs have been evaluated as heterogeneous Lewis acid catalysts for chemical conversion of CO_2, the catalytic processes usually require either high temperature and/or pressure to achieve good reaction yields,[8] or the presence of co-catalysts such as nBu$_4$NBr (TBAB), which is considered to be an environmentally unfriendly reagent.[9] The underlying cause of this low activity could be the low density of Lewis acid active sites in these MOF materials. One way to overcome this is to increase the density of Lewis acid active sites by decorating the vertexes, and/or edges, and/or faces of polyhedral cages in MOFs with catalytically active centers.[10] For example, Ma et al. have succeeded in raising the density of catalytically active sites by substitution of the facial ligand in the cage of MOF-505 with a metalloporphyrin ligand.[10a] The modified cuboctahedral cage shows high catalytic activity for the cycloaddition of CO_2 and epoxide under ambient conditions, with twice the efficiency of its prototypal MOF-505.[10a] However, a co-catalyst TBAB was still needed in this case. Herein, we report a novel 3D→3D

[a] *State Key Laboratory of Structural Chemistry, Fujian Institute of Research on the Structure of Matter, Chinese Academy of Sciences, Fuzhou, Fujian 350002, P. R. China. E-mail: swdu@fjirsm.ac.cn. Fax: 86-591-83709470*

[b] *Graduate University of Chinese Academy of Sciences, Beijing 100039, P. R. China.*

[c] *College of Chemistry, Fuzhou University, Fuzhou 350001, P. R. China.*

interpenetrated Zn-polyhedral MOF, $[Zn_6(TATAB)_4(DABCO)_3(H_2O)_3]\cdot12DMF\cdot9H_2O$ (**1**) (H_3TATAB = 4,4',4''-*s*-triazine-1,3,5-triyl-tri-*p*-aminobenzoic acid, DABCO = 1,4-diazabicyclo[2.2.2]octane) based on a dual-walled Zn_{48} cage. The high density of Lewis acid active sites in the dual-walled cage and the enriched CO_2-philic groups in the ligand enable **1** to function as efficient catalyst for the cycloaddition of propylene oxide with CO_2 into propylene carbonate under mild and co-catalyst free conditions.

Experimental section

General information

All reagents were commercially purchased and used without any further purification. The purity of all gases is 99.999%. The TGA were performed on a TGA/NETZSCH STA449C instrument heated from 40 to 800ºC under a nitrogen atmosphere at a heating rate of 10°C/min. Powder X-ray diffraction was recorded on a PANalytical X'pert PRO X-ray Diffraction using Cu-Kα radiation in the 2θ range of 5–50°. The Fourier transform infrared spectra using KBr pellets were collected on a Spectrum-One FT-IR spectrophotometer in the range of 4000–400 cm^{-1}. Elemental analyses (C, H, N) were measured with an Elemental Vairo EL III Analyser. Gas adsorption measurement was performed in the ASAP (Accelerated Surface Area and Porosimetry) 2020 System. Gas chromatography (GC) measurements were analysed using a GC-Smart (SHIMADZU) spectrometer and a flame ionization detector (FID). Products were checked by Gas Chromatography-Mass Spectrometry 4000GC-MS (Varian-Agilent).

Preparation of $[Zn_6(TATAB)_4(DABCO)_3(H_2O)_3]\cdot12DMF\cdot9H_2O$ (1)

A mixture of $Zn(NO_3)_2\cdot6H_2O$ (0.60 mmol, 178.20 mg), H_3TATAB (0.45 mmol, 218.25 mg) and DABCO (0.3 mmol, 66.06 mg) was sealed in a 20 mL of Teflon-lined stainless steel vessel with 6 mL of *N*,*N*'-dimethylformamide (DMF). The mixture was heated to 115°C in 4 hours and kept at this temperature for 3 days. Then the reaction system was cooled slowly to room temperature during another 3 days. The colorless cubic crystals of **1** were collected, washed with DMF and CH_2Cl_2 and dried in air (yield 85% based on $Zn(NO_3)_2\cdot6H_2O$). Elemental analysis calcd. (%) for **1** $C_{150}H_{204}N_{42}O_{48}Zn_6$ (3755.79): C 47.97, H 5.47, N 15.66; found: C 47.89, H 5.22, N 15.45. FT-IR (KBr, cm^{-1}) (see supporting information Fig. S1): 3289s, 1602s, 1490s, 1377vs, 1305s, 1244s, 1176s, 1053w, 1014w, 918w, 898w, 860s, 802s, 786s, 734w, 705w, 619w, 595w, 568w, 507w, 470w, 424w.

Single-crystal X-ray Diffraction Study

Single-crystal X-ray diffraction data were collected on a Rigaku Diffractometer with a Mercury CCD area detector (Mo Kα: λ = 0.71073 Å) at room temperature. Crystal Clear software was used for data reduction and empirical absorption correction. The structure was solved by direct method using SHELXTL and refined by full-matrix least-squares on F^2 using SHELX-97 program.[11a] Metal atoms in the compound were located from

the *E*-maps, and other non-hydrogen atoms were located in successive difference Fourier syntheses. All non-hydrogen atoms were refined anisotropically. The organic hydrogen atoms were positioned geometrically. The cavities were filled with highly disordered lattice solvent molecules that could not be completely mapped by single-crystal X-ray diffraction, which is often observed in high-symmetry structures.[12] Thus SQUEEZE routine of PLATON was applied to remove contributions to scattering from solvent molecules. In addition, because some atoms (C1, C2) of DABCO lie in the special position, the atoms are statistical distribution in the special position. The reported refinements are of guest-free structure by SQUEEZE routine.[11b] The final formula of **1** was calculated from the squeeze result combined with the elemental analysis and TGA data. The elemental analysis suggests that there are 48 DMF and 36 H_2O molecules located in the cavity per unit cell (2280 electrons) which is well consistent with the squeeze result (2303 electrons calculated using Platon Software). Also, the formula can be further supported by the TGA results (*vide infra*). Crystallographic data and other pertinent information for **1** are summarized in Table S2. CCDC number for **1** is 1450479.

General procedure for the cycloaddition of CO_2 to cyclic carbonate catalysed by 1.

In a 50 mL stainless-steel autoclave with a magnetic stirring bar in the absence of solvent and co-catalyst under CO_2 pressure with catalyst 0.21 or 0.42 mol% per paddlewheel units (desolvation and dehydration under vacuum at 120°C) and epoxides (20 mmol) were added. The reaction was carried out at 1 atm CO_2 and conducted for the appropriate time upon heating at 100°C. The reuse experiments were carried out for the cycloaddition of propylene oxide with CO_2 under similar conditions. The catalyst was retrieved by filtration, washed and soaked with DMF and CH_2Cl_2 (*ca*. 5 × 10 mL), and reactivated as above prior to being used for the next catalytic cycle. Products were monitored by GC–Smart (DM-1 column, L x I. D. 30 m x 0.25 µm; injector temperature 220°C) and identified by the comparison of GC retention times and mass spectra with those of the authentic samples. All the yields were based on epoxide.

Results and discussion

Colorless cubic crystals of **1** were prepared under solvothermal conditions *via* the reaction of $Zn(NO_3)_3\cdot6H_2O$ salt with the organic linkers H_3TATAB and DABCO at 115°C in DMF. Single crystal X-ray diffraction study reveals that **1** crystallizes in the highly symmetric cubic space group *Im*-3. The asymmetry unit of **1** consists of two quarters of Zn^{2+} ion, one third of a TATAB^{3-} ligand and one fourth of a DABCO and a coordinated water molecule. It also contains 3/4 DMF and 3/4 water solvent molecule, as determined by CHN elemental analysis and TGA results. The two crystallographic independent Zn^{2+} ions both adopt a square pyramidal coordination geometry with the basal plane being occupied by four carboxylate oxygen atoms and the apical position being taken by a nitrogen atom from

DABCO in Zn1 or a coordinated water molecule in Zn2 (see supporting information Fig. S2). The Zn1 and Zn2 atoms are bridged by four bridging carboxylate groups from four different TATAB^{3-} ligands, forming a {Zn$_2$(O$_2$C)$_4$} paddlewheel secondary building unit (SBU) with a short Zn–Zn distance of 2.94 Å.

The most fascinating topological feature of **1** is the dual-walled cage motif, in which one cage is encapsulated by another cage (Fig. 1c), a result from the interpenetration of two independent but identical 3D cage nets. Compound **1** is built from a icosahedral Zn$_{24}$ cage (denoted as Zn$_{24}$-A) where the paddlewheel {Zn$_2$(O$_2$C)$_4$} dimers residue at its twelve vertexes and TATAB^{3-} ligands occupy eight of the twenty trigonal planes (Fig. 1a). The cubic packing of non-space-filling icosahedral cages through face- and edge-sharing creates anther Zn$_{24}$ cage (denoted as Zn$_{24}$-B) in the gap of each eight neighbouring Zn$_{24}$-A cages. Compared to Zn$_{24}$-A, the Zn$_{24}$-B cage is also defined by twelve {Zn$_2$(O$_2$C)$_4$} dimers and eight TATAB^{3-} ligands, except that six pairs of adjacent {Zn$_2$(O$_2$C)$_4$} vertices each is further connected by an additional DABCO ligand, resulting in a highly distorted icosahedral cage (Fig. 1b).
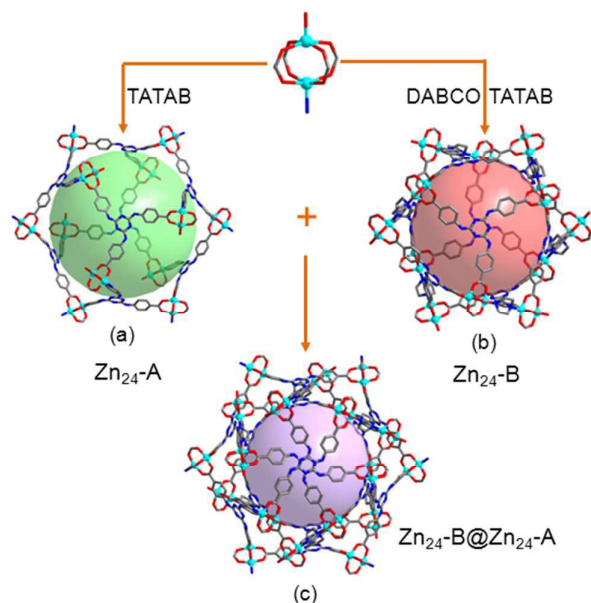

Fig. 1 (a) View of the Zn$_{24}$-A cage (the distance between opposite vertices is *ca.* 34.4 Å). (b) View of the Zn$_{24}$-cage (the distance between opposite vertices is *ca.* 30.2 Å). (c) View of the dual-walled cage motif of **1**.

Further analysing the structure of **1** reveals that these two types of cages are alternatively arranged to form a 3D network in which each cage of one type is encircled by eight cages of the other type and *vice versa* (Fig. 2a, 2b). Two identical 3D cage networks are interpenetrated in such a complicated way that every Zn$_{24}$-B cage in one net is completely encapsulated by a Zn$_{24}$-A cage of the other net and *vice versa*, resulted in a 3D framework with double-walled cages (Fig. 2c). Remarkably, each Zn$_{24}$-A cage in one net is interlaced to eight Zn$_{24}$-A cages belonging to the other net through all its ligand-decorated trigonal planes, that is, each ligand defined plane of one Zn$_{24}$-A

cage is interlocked by another Zn$_{24}$-A cage with face-to-face π-π interactions between the central cores of TATAB^{3-} ligands stacked in an eclipsed fashion (centroid-to-centroid distance: 3.412). The propagation of octuplet polycatenation leads to a 3D extended polyhedral architecture of **1**, which is one of the rare examples of 3D polycatenanes by mechanically linking coordination cages,[13] and is the second example that also features a cage-within-cage motif.[13f]
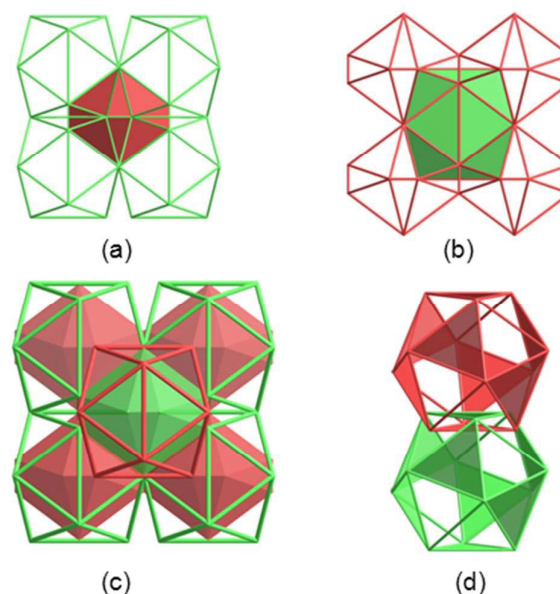

Fig. 2 (a) View of the Zn$_{24}$-B (pink polyhedron) generated by eight Zn$_{24}$-A cages. The other four Zn$_{24}$-A cages behind are not shown. (b) View of the Zn$_{24}$-A cage generated by eight Zn$_{24}$-B cages. The other four Zn$_{24}$-B cages behind are not shown. (c) The interpenetration of two identical nets of **1**, a showing cage-within-cage motif. (d) One of the octuplet catenation showing the interlocking between two Zn$_{24}$-A coming from different nets.

In **1**, the dual-walled cage is ca. 3.2 nm in diameter and each contains 48 Zn^{2+} Lewis acid catalytic sites and 48 -NH- Lewis base sites that are able to interact with CO$_2$. The combination of high density of catalytic sites and CO$_2$-philic groups in **1** may guarantee an outstanding CO$_2$ chemical fixation performance. Removal of the guest molecules reveals that the effective free volume of **1**, calculated by PLATON analysis, is 64.5% of the crystal volume (15175.9 Å^3 of the 23534.6 Å^3 unit cell volume). The phase purity of **1** was checked by powder XRD recorded at room temperature (see supporting information Fig. S3). The peak positions of the simulated pattern closely match those of the experimental ones, indicating phase purity of the as-synthesized sample. The TGA and variable temperature XRD measurements were performed to study the thermal stability of **1**. The TGA curve of **1** shows a continual weight loss without an obvious plateau from 40 to 500 °C (see supporting information Fig. S4). After removing the lattice solvents by treating **1** under vacuum at 150 °C for 24 hours, the TGA curve of the desolvated sample shows almost no weight loss from 0 to *ca.* 300 °C. Thus, the weight loss of 27.1% from 0 to 300 °C corresponds to the loss of lattice DMF and water molecules (calcd. 27.6%). The variable temperature XRD experiment also

indicates that **1** is stable up to *ca*. 200 °C, above this temperature, the framework starts to decompose (see supporting information Fig. S3).

The permanent porosity of **1** was evaluated by measuring N_2 adsorption isotherms at 77 K using activated materials. The resulting N_2 isotherms exhibited typical type I behaviour, indicative of microporosity (see supporting information Fig. S5). From the isotherm, the BET/Langmuir surface area for **1** was estimated to be 61.4/87.4 m^2 g^{-1}. Single-component gas adsorption isotherms (CO_2 and N_2) were measured at 273 K for **1**. Compound **1** displays a high CO_2 capacity (49.1 cm^3 g^{-1}) at 769 mmHg and 273 K (see supporting information Fig. S6). This is in contrast to the N_2 uptake capacity observed for **1** (5.3 cm^3 g^{-1}) at the same temperature and pressure. Furthermore, the initial uptake in the low-pressure region of the CO_2 isotherm at 273 K is much steeper than that observed for N_2. These results indicate the high affinity to CO_2 of the MOF framework, which demonstrates the potential of the MOF for CO_2 physisorption and CO_2/N_2 separation. The high CO_2 uptake of **1** is due to the strong hydrogen bonding between the NH group of TATAB[3−] ligand and CO_2 molecule.[14]

**Table 1** Various conditions for converting CO_2 into cyclic carbonate [a]

Entry	Catalyst (amt (mol%))	T (°C)	P (atm)	t (h)	Conv. (%)	Yield[b] (%, based on epoxide)
1	1 (0.42)	100	1	16	100	99
2	1 (0.42)	100	10	1	100	99
3	1 (0.21)	100	10	6	99	98
4	1 (0.42)	100	1 (P_{N2}/P_{CO2}= 8/2)	16	30	28
5	1 (0.42)	100	1 (P_{N2}/P_{CO2}= 2/8)	16	70	67
6	blank	100	1	16	--	--

[a] Reaction conditions: epoxide (20.0 mmol) with catalyst per paddlewheel units; [b] The yields were determined by GC with *n*-butanol as an internal standard.

Given that **1** possess high density of Lewis acid sites and excellent affinity to CO_2, we decide to investigate the catalytic capability of **1** as Lewis acid catalyst for the cycloaddition of CO_2 with epoxides to form cyclic carbonates. As shown in Table 1, compound **1** demonstrates highly efficient catalytic activity for cycloaddition of propylene oxide with CO_2 into propylene carbonate at 100 °C under 1 atm CO_2 pressure with a yield of 99% over 16 h without any co-catalyst (Table 1, entry 1). At 10 atm CO_2 pressure, the reaction completes in only one hour but finishes in six hours if half the amount of catalyst is used (Table 1, entry 2, 3). In view of the fact that **1** has a high affinity for CO_2 and a low affinity for N_2, we also carried out the catalytic reaction under simulated dry flue-gas conditions. When the pressure ratio of N_2 and CO_2 is 8/2 and the total pressure is 1

atm, the yield of propylene carbonate is 28% (Table 1, entry 4). But when the pressure ratio of N_2 and CO_2 is 2/8, the yield of propylene carbonate is 67% (Table 1, entry 5). These results indicate again that **1** can selectively absorb CO_2 over N_2 and the presence of N_2 has little interference in the chemical fixation of CO_2. In the absence of compound **1**, no propylene carbonate was found (Table 1, entry 6). Significantly, the catalytic reaction is environmental friendly as no co-catalyst and solvent was needed and the reaction was carried out at milder conditions compared to other MOF systems (Table S1).

Table 2 Various carbonates from different epoxides catalysed by **1** [a]

Entry	Epoxides	Products	Conv. (%)	Yield[b] (%, based on epoxides)	TON [c]
1			100	99	246
2			98	95	158
3			92	91	152
4			90	89	148
5			50	50	83
6			8	8	13

[a] Reaction conditions: epoxides (20.0 mmol), **1** (0.42 mol% per paddlewheel units), CO_2 (1 atm), 100 °C and 16 hours; [b] The yields were determined by GC with *n*-butanol as an internal standard; [c] TON = moles of aimed product/moles of active metal sites.

The excellent catalytic activity of **1** for the chemical fixation of CO_2 encouraged us to further explore the generality of this catalytic system. Chemical fixation of CO_2 with epoxides substituted with different functional groups under similar conditions was investigated (Table 2). A high catalytic activity was observed for the cycloaddition of epichlorohydrin and butylene oxide with CO_2 into butylene carbonates at 100 °C and 1 atm CO_2 pressure with yields of 95% and 91%, respectively over 16 h (Table 2, entry 2 and 3). Even for the large styrene oxide, the yield of the cycloaddition is still up to 89% (Table 2, entry 4). However, further increasing the size of epoxide substrates resulted in a dramatic decrease in the yield of cyclic carbonates. The yields of cycloaddition were dropped down to 50% (Table 2, entry 5) and 8% (Table 2, entry 6) for benzyl phenyl glycidyl ether and *trans*-2,3-diphenylethylene oxide. It is speculated that the limited diffusion of the large-sized epoxide substrate into the void space within the dual-walled cage of **1** is responsible for these low yields. [13e, 15, 16]

In addition to high catalytic activity, the reusability and stability are also very important for heterogeneous catalytic

systems. The recycling experiments were conducted using **1** as catalyst in the cycloaddition of propylene oxide with CO_2 under similar conditions. The catalyst after one cycle can be easily recovered by centrifugation and subsequently used in the successive runs for six cycles without an appreciable loss of its catalytic performance (Fig. 3). A 96% yield of cyclic carbonate was obtained in the sixth run. The powder XRD of the recovered catalyst was identical to that of the freshly prepared sample, indicating the stability of **1** during the catalytic reaction (see supporting information Fig. S7). The reusability of **1** was also tested through recycle reaction kinetics for the first and second cycle (see supporting information Fig. S8). In both reaction cycles, similar activities are clearly exhibited. To confirm the heterogeneous nature of **1**, the catalytic reaction was stopped after 3 hours and the reaction mixture was filtered while still hot to remove the catalyst. The reaction was then continued for another 13 hours, during which the yield of propylene carbonate remained unchanged (see supporting information Fig. S8).
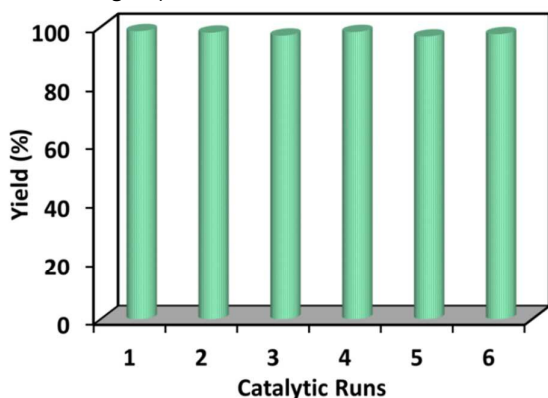

Fig. 3 The catalytic cycles of compound **1** for the cycloaddition of CO_2 and propylene epoxide reaction.

Besides to the high density of Lewis acid active sites, the good catalytic activity of **1** may also be attributed to the existence of amine-functionalized ligands. Previous research has shown that the introduction of Lewis basic functional groups such as amines into MOFs can not only increase the CO_2 affinity but also improve the carbonate yields due to the synergistic effect of the Lewis acid-base pair.[17] Accordingly, a tentative mechanism can be proposed for the cycloaddition of epoxide and CO_2 into cyclic carbonate catalysed by **1** bearing acid-basic pair. First, CO_2 is activated at the basic amine sites forming a carbamate species, which then reacts with epoxides that are adsorbed on the adjacent Zn^{2+} Lewis acidic sites to form ring opening intermediate. Second, ring-closure through an intramolecular nucleophilic attack by the oxy anion at the carbon center of CO_2 occurs to generate a cyclocarbonate.

Conclusions

In summary, we have synthesized a 3D→3D interpenetrated polyhedral MOF featuring a fascinating cage-within-cage motif and a rarely observed octuplet polycatenation. Due to the high density of Lewis acid sites and the excellent affinity to CO_2 of the cage, compound **1** exhibits good performance for the cycloaddition of propylene oxide with CO_2 into propylene carbonate under mild temperature and 1 atm CO_2 pressure with a yield of 99% over 16 h. Furthermore, it is the first MOF that is able to catalyse cycloaddition of CO_2 to epoxides under mild and solvent-free conditions without the help of any co-catalyst.

Notes and references

1   (a) M. Ed. Aresta, Carbon Dioxide as Chemical Feedstock; *WileyVCH: Weinheim*, Germany, 2010; (b) I. Omae, *Catal. Today*, 2006, **115**, 33–52.
2   (a) A. Goeppert, M. Czaun, G. K. S. Prakash, G. A. Olah, *Energy Environ. Sci.*, 2012, **5**, 7833–7853; (b) A. Kumar, D. G. Madden, M. Lusi, K. J. Chen, E. A. Daniels, T. Curtin, J. J. Perry IV, M. J. Zaworotko, *Angew. Chem. Int. Ed.*, 2015, **54**, 14372–14377; (c) X. C. Kang, Q. G. Zhu, X. F. Sun, J. Y. Hu, J. L. Zhang, Z. M. Liu, and B. X. Han, *Chem. Sci.*, 2016, **7**, 266–273; (d) Z. H. He, Q. L. Qian, J. Ma, Q. L. Meng, H. C. Zhou, J. L. Song, Z. M. Liu, and B. X. Han, *Angew. Chem. Int. Ed.*, 2016, **55**, 737–741.
3   (a) M. Yoshida, and M. Ihara, *Chem. Eur. J.*, 2004, **10**, 2886 – 2893; (b) D. J. Darensbourg, *Chem. Rev.*, 2007, **107**, 2388–2410; (c) J. Whiteoak, N. Kielland, V. Laserna, E. C. Escudero-Adan, E. Martin, and A. W. Kleij, *J. Am. Chem. Soc.*, 2013, **135**, 1228–1231; (d) M. North, R. Pasquale, and C. Young, *Green Chem.*, 2010, **12**, 1514–1539; (e) J. Ma, J. L. Song, H. Z. Liu, Z. F. Zhang, T. Jiang, H. L. Fan, and B. X. Han, *Green Chem.*, 2012, **14**, 1743–1748; (f) P. Pescarmona, and M. Taherimehr, *Catal. Sci. Technol.*, 2012, **2**, 2169–2187; (g) T. Ema, Y. Miyazaki, S. Koyama, Y. Yano, and T. Sakai, *Chem. Commun.*, 2012, **48**, 4489–4491; (h) B. Schaffner, F. Schäffner, S. P. Verevkin, and A. Börner, *Chem. Rev.*, 2010, **110**, 4554–4581.
4   (a) A. Decortes, A. M. Castilla, and A. W. Kleij, *Angew. Chem. Int. Ed.*, 2010, **49**, 9822–9837; (b) M. North, and R. Pasquale, *Angew. Chem. Int. Ed.*, 2009, **48**, 2946–2948; (c) X. B. Lu, B. Liang, Y. J. Zhang, Y. Z. Tian, Y. M. Wang, C. X. Bai, H. Wang, and R. Zhang, *J. Am. Chem. Soc.*, 2004, **126**, 3732–3733; (d) M. Mikkelsen, M. Jørgensen, and F. C. Krebs, *Energy Environ. Sci.*, 2010, **3**, 43–81; (e) H. Yasuda, L. N. He, T. Sakakura, and C. Hu, *J. Catal.*, 2005, **233**, 119–122; (f) T. Sakakura, J. C. Choi, and H. Yasuda, *Chem. Rev.*, 2007, **107**, 2365–2387; (g) M. R. Kember, A. Buchhard, and C. K. Williams, *Chem. Commun.*, 2011, **47**, 141–163; (h) T. Sakakura, and K. Kohno, *Chem. Commun.*, 2009, 1312–1330.
5   (a) K. Yamaguchi, K. Ebitani, T. Yoshida, H. Yoshida, and K. Kaneda, *J. Am. Chem. Soc.*, 1999, **121**, 4526–4527; (b) E. J. Doskocil, S. V. Bordawekar, B. C. Kaye, and R. J. Davis, *J. Phys. Chem. B*, 1999, **103**, 6277–6282; (c) T. Yano, H. Matsui, T. Koike, H. Ishiguro, H. Fujihara, M. Yoshihara, and T. Maeshima, *Chem. Commun.*, 1997, 1129–1130; (d) H. Yasuda, L. N. He, T. Sakakura, *J. Catal.,* 2002, **209**, 547–550;

(e) Y. Xie, T. T. Wang, X. H. Liu, K. Zou, W. Q. Deng, *Nat. Commun.,* 2013, **4**, 1960–1966.

6 (a) B. Wang, A. P. Côté, H. Furukawa, M. O'Keeffe, O. M. Yaghi, *Nature*, 2008, **453**, 207–211; (b) H. Furukawa, N. Ko, Y. B. Go, N. Aratani, S. B. Choi, E. Choi, A. Ő. Yazaydin, R. Q. Snurr, M. O'Keeffe, J. Kim, O. M. Yaghi, *Science*, 2010, **329**, 424–428; (c) Y. B. He, W. Zhou, G. D. Qian, B. L. Chen, *Chem. Soc. Rev.*, 2014, **43**, 5657–5678; (d) J. R. Li, R. J. Kuppler, H. C. Zhou, *Chem. Soc. Rev.*, 2009, **38**, 1477–1504; (e) D. P. Broom, K. M. Thomas, *MRS Bull.*, 2013, **38**, 412–421; (f) W. M. Xuan, C. F. Zhu, Y. Liu, Y. Cui, *Chem. Soc. Rev.*, 2012, **41**, 1677–1695.

7 (a) W. Y. Gao, S. Q. Ma, *Comments Inorg. Chem.*, 2014, **34**, 125-141; (b) J. W. Liu, L. F. Chen, H. Cui, J. Y. Zhang, L. Zhang, C. Y. Su, *Chem. Soc. Rev.*, 2014, **43**, 6011-6061.

8 (a) A. C. Kathalikkattil, D. W. Kim, J. Tharun, H. G. Soek, R. Roshan, and D. W. Park, *Green Chem.*, 2014, **16**, 1607–1616; (b) D. A. Yang, H. Y. Cho, J. Kim, S. T. Yang, and W. S. Ahn, *Energy Environ. Sci.*, 2012, **5**, 6465–6473; (c) W. Y. Gao, L. Wojtas, and S. Q. Ma, *Chem. Commun.*, 2014, **50**, 5316–5318; (d) B. Zou, L. Hao, L. Y. Fan, Z. M. Gao, S. L. Chen, H. Li, C. W. Hu, *J. Catal.*, 2015, **329**, 119–129. (e) Z. Zhou, C. He, J. H. Xiu, L. Yang, C. Y. Duan, *J. Am. Chem. Soc.*, 2015, **137**, 15066–15069.

9 (a) X. Q. Huang, Y. F. Chen, Z. G. Lin, X. Q. Ren, Y. N. Song, Z. Z. Xu, X. M. Dong, X. G. Li, C. W. Hu, and B. Wang, *Chem. Commun.*, 2014, **50**, 2624–2627; (b) D. X. Ma, B. Y. Li, K. Liu, X. L. Zhang, W. J. Zou, Y. Q. Yang, G. H. Li, Z. Shi, and S. H. Feng, *J. Mater. Chem. A*, 2015, **3**, 23136–23142; (c) J. L. Song, Z. F. Zhang, S. Q. Hu, T. B. Wu, T. Jiang, and B. X. Han, *Green Chem.*, 2009, **11**, 1031–1036; (d) O. V. Zalomaeva, A. M. Chibiryaev, K. A. Kovalenko, O. A. Kholdeeva, B. S. Balzhnimaev, and V. P. Fedin, *J. Catal.*, 2013, **298**, 179–185; (e) w. Kleist, F. Jutz,M. Maciejewski, and A. Baiker, *Eur. J. Inorg. Chem.,* 2009, **2009**, 3552–3561; (f) H. Y. Cho, D. A. Yang, J. Kim, S. Y. Jeong, and W. S. Ahn, *Catal. Today*, 2012, **185**, 35–40; (g) X. Zhou, Y. Zhang, X. G. Yang, L. Z. Zhao, and G. Y. Wang, *J. Mol. Catal. A: Chem.,* 2012, **361–362**, 12–16; (h) C. M. Miralda, E. E. Macias, M. Q. Zhu, P. Ratnasamy, and M. A. Carreon, *ACS Catal.*, 2012, **2**, 180–183.

10 (a) W. Y. Gao, Y. Chen, Y. H. Niu, K. Williams, L. Cash, P. J. Perez, L. Wojtas, J. F. Cai, Y. S. Chen, and S. Q. Ma, *Angew. Chem. Int. Ed.*, 2014, **126**, 2653–2657; (b) G. R. Desiraju, *Angew. Chem. Int. Ed.*, 2007, **46**, 8342–8356; (c) J. J. Perry IV, J. A. Perman, and M. J. Zaworotko, *Chem. Soc. Rev.*, 2009, **38**, 1400–1417; (d) S. T. Zheng, T. Wu, B. Irfanoglu, F. Zuo, P. Y. Feng, and X. H. Bu, *Angew. Chem.*, 2011, **123**, 8184–8187; *Angew. Chem. Int. Ed.*, 2011, **50**, 8034–8037.

11 (a) G. M. Sheldrick, *SHELXL-97 Program for X-ray Crystal Structure Refinement*, University of Göttingen, Germany, 1997. (b) A. L. Spek, *PLATON-97*; University of Utrecht: Utrecht, The Netherlands, 1997.

12 (a) S. T. Zheng, T. Wu, F. Zuo, C. S. Chou, P. Y. Feng, X. H. Bu, *J. Am. Chem. Soc.*, 2012, **134**, 1934–1937; (b) X. S. Wang, L. Meng, Q. G. Cheng, C. Kim, L. Wojtas, M. Chrzanowski, Y. S. Chen, X. P. Zhang, S. Q. Ma, *J. Am. Chem. Soc.,* 2011, **133**, 16322–16325.

13 (a) X. Kuang, X. Wu, R. Yu, J. P. Donahue, J. Huang, C. Z. Lu, *Nat. Chem.*, 2010, **2**, 461-465; (b) J. Heine, J. Schmedt auf der Günne, S. Dehnen, *J. Am. Chem. Soc.*, 2011, **133**, 10018-10021; (c) L. Jiang, P. Ju, X. R. Meng, X. J. Kuang, T. B. Lu, *Sci. Rep.*, 2012, **2**, 668-772; (d) S. Ma, X. S. Wang, D. Yuan, H. C. Zhou, *Angew. Chem. Int. Ed.*, 2008, **47**, 4130-4133; (e) Y. Shen, H. B. Zhu, J. Hu, Y. Zhao, *CrystEngComm.*, 2015, **17**, 2080–2082. (f) Y. H. Han, C. B. Tian, P. Lin, and S. W. Du, *J. Mater. Chem. A,* 2015, **3**, 24525-24531.

14 (a) A. Khutia, C. Janiak, *Dalton Trans.*, 2014, **43**, 1338–1347; (b) N. Planas, A. L. Dzubak, R. Poloni, L. C. Lin, A. McManus, T. M. McDonald, J. B. Neaton, J. R. Rong, B. Smit, L. Gagliardi, *J. Am. Chem. Soc.*, 2013, **135**, 7402–7405; (c) S. Pal, A. Bhunia, P. P. Jana, S. Dey, J. Möllmer, C. Janiak, H. P. Nayek, *Chem. Eur. J.*, 2015, **21**, 2789–2792.

15 (a) N. W. Ockwig, O. Delgado-Friedrichs, M. O'Keeffe, O. M. Yaghi, *Acc. Chem. Res.*, 2005, **38**, 176–182.

16 Y. Chen, V. Lykourinou, T. Hoang, L. J. Ming, and S. Ma, *Inorg. Chem.*, 2012, **51**, 9156–9158.

17 (a) T. Lescouet, C. Chizallet, and D. Farrusseng, *Chemcatchem,* 2012, **4**, 1725–1728; (b) Y. J. Kim and D. W. Park, *J. Nanosci. Nanotechnol.*, 2013, **13**, 2307–2312; (c) R. Srivastava, D. Srinivas, P. Ratnasamy, *Microporous Mesoporous Mater.,* 2006, **90**, 314–326.